System Performance of Self-Organizing Network Algorithm in WiMAX Femtocells (Invited Paper)

Hui Zeng, Chenxi Zhu and Wei-Peng Chen
Fujitsu Laboratories of America
{hui.zeng, chenxi.zhu, wei-peng.chen}@us.fujitsu.com

ABSTRACT
Femtocell is an emerging idea in the next generation wireless networks to enhance the indoor coverage. One of challenges of femtocell is how to configure femto base stations (fBSs) in an autonomous and optimal manner. In this paper, we evaluate performance of the WiMAX (802.16e) femtocell systems, in terms of the network coverage and the system capacity. Particularly we are interested in the performance of Mobile Stations (MSs) in the indoor environment. The single-segment systems, where all fBSs are assigned the same frequency segment, are considered at first. Through extensive simulation, we investigate the effect of the TX power at fBSs, cell radius and loading factor. Furthermore, several heuristic frequency assignment schemes are proposed and compared along with the random assignment scheme that randomly assigns one of three segments for each fBS. Finally, Least Interference Power (*LIP*) scheme, which for an fBS picks the segment with the least total interference power received at this fBS, is recommended due to its complete locality, practical metric, the least computation and close-to-optimum performance.

Categories and Subject Descriptors
C.2.1 [**Computer-Communication Networks**]: Network Architecture and Design – *wireless communication.*
C.4 [**Performance of Systems**]: *design studies, modeling techniques, performance attributes.*

General Terms
Algorithms, Management, Performance, Design.

Keywords
Femtocell, WiMAX, 802.16, Frequency Assignment, Network Coverage, Network Capacity.

1. INTRODUCTION
Systems based on IEEE 802.16 standard (mobile WiMAX, or 802.16e) is one of the leading candidates for 4G wireless systems. One of the biggest challenges for mobile WiMAX with macrocell size, however, is to provide mobile coverage and high data rate to one of the most demanding environments – inside building – in a cost-efficient way. One of the solutions is to deploy the smaller size base stations (BS), such as picocell or femtocell BSs (fBSs). The emerging femtocell solution offers benefits to both operators and consumers. For operators, the overall system capacity is increased because of better coverage and part of traffic redirected to the backhaul connection of fBS through consumers' broadband connections. For consumers, the fBS provides the enhanced service coverage covering the area of house or small business office. Consumers experience the same quality of service both inside and outside their home. In other words, femtocell is one type of realizations of fixed-mobile convergence (FMC).

One of main challenges in femtocell networks is how to configure fBSs in an autonomous and optimal manner. Since fBSs are considered as consumer devices which are installed by end users, autonomous configuration is absolutely necessary. Moreover, numerous fBSs are installed by users at their homes without precise plan as macro base stations. Therefore, a self-organizing network (SON) algorithm is very important for femtocells. SON algorithm intends to configure fBSs autonomously and alleviate operators' management efforts. In addition, the system parameters are properly setup to achieve minimal interference and thus maximal system capacity of femtocells.

In this paper, we report a detailed system level performance evaluation for mobile WiMAX systems with femtocells. Our simulation methodology follows what specified by WiMAX Forum [1]. Particularly we consider only Down Link (DL) and the indoor users (mobile stations, or MSs). We first study the single-segment systems with all fBSs in the same frequency segment. The effect of the TX power at fBSs, cell radius and loading factor (defined as the percentage of subchannels in the assigned frequency segment that is actually used by the fBS), are investigated. We calculate effective Carrier to Interference-plus-Noise Ratio (CINR) for the indoor MSs, under detailed channel models using Exponential Effective Signal-to-Interference-Ratio Mapping (EESM) method, as the basis for system coverage and capacity analysis. PHY and MAC overhead are not explicitly simulated and therefore included in system capacity.

The modeling and performance evaluation of femtocell systems have recently been conducted in [2, 3, 4, 5, 6]. In [2], 1.9 GHz path loss models are derived from measurements for Line-of-Sight or Non-Line-of-Sight (LOS/NLOS) links in microcell size. For LOS links, the power law exponent n after the break-point distance (d_{BP}) is estimated to be varying from 3.29 to 4.16. The measured data and empirical models for 2.5 GHz path loss and multipath delay spread in femtocell size are presented in [3, 4].

WICON'08, November 17–19, 2008, Maui, Hawaii, USA.

Digital Object Identifier: 10.4108/ICST.WICON2008.4915
http://dx.doi.org/10.4108/ICST.WICON2008.4915

And in the models without d_{BP}, n is estimated to be 2.4. Furthermore, the partition-dependant attenuation factors are introduced to path loss models in [3, 4, 5] for site-specific propagation effects, such as reflection, diffraction, or penetration losses caused by a particular building layout, construction materials, furniture, etc. It is demonstrated that the partition-based model works fine for short TX-RX distance with a small number of multi-path scatters. In [5], the indoor picocell environment with square room cubicles of 10x10 m^2 has been considered for the system level performance evaluation. Its empirical results of the parameters in the wireless channel models, although in 2 GHz, can be borrowed in our 2.5 GHz femtocell models.

Frequency (segment) assignment schemes, also known as dynamic channel assignment (DCA) strategies, have been investigated in the literature to achieve improved system performance and "self-organizing" within the network [7, 8, 9, 10, 11]. In the above literature, several frequency assignment schemes and the variations are proposed including: Minimum Reuse Distance, Optimization-based, First Available, Mean Square Distance, Nearest Neighbor, Frequency Exhaustive, Node Ordering, etc. The First Available scheme, a simple scheme with which the first available channel found during the search is assigned, is shown in [7] to perform closely to some of the more complicated schemes. It has also been proven in [11] that the optimization problem for channel assignments is NP-hard, through transformation to the generalized graph coloring problem.

We focus on the self-organizing of WiMAX femtocell network, where the frequency assignment decisions are performed by a centralized network controller. In the femtocell SON scheme, the fBS conducts measurements and reports results to the network controller. The network controller assigns the frequency segment to an fBS based on the reports of measurement results and the frequency assignments that have been made in its adjacent femtocells. An overview of self-organization is presented in [12] in the context of communications and computer networks. In this paper, we propose several heuristic greedy-based schemes in the SON architecture and evaluate their performance. The Random Scheme, which randomly assigns one of three segments for each fBS, is the simplest scheme and serves as a comparison basis.

The rest of this paper is organized as follows: Section 2 presents our system configuration, cell layout, channel models and our DL CINR calculation with EESM method. The simulation results under different system parameters are shown in Section 3 for the single-segment systems where all fBSs are assigned the same frequency segment. In Section 4, different frequency assignment schemes are introduced and their performances are compared as well. Finally, Section 5 summarizes the paper.

2. SYSTEM MODELS

In each frame, there are 47 data symbols and 30 subchannels in total. The DL and UL (Up Link) partitioning in a frame is 2:1. For simplicity, our system simulation focuses on the DL with PUSC (partial usage of subchannels) [13] because similar result is expected on the UL.

2.1 Femtocell WiMAX System Configuration

We list the configuration of the femtocell WiMAX network and DL OFDMA parameters in Table 1.

Table 1. WiMAX system and DL OFDMA parameters

Parameters		Value
Number of Cells in Regular Grid		25 (5x5)
Operating Frequency		2500 MHz
Duplex		TDD
fBS-to-fBS Distance		10 ~ 80 m
fBS/MS Antenna		Omni-directional, –1dBi
fBS/MS Diversity Antenna Gain		3dB
fBS TX Power		14/17/23 dBm
fBS/MS Noise Figure		5dB / 7dB
Implementation Loss at RX		5dB
MS Speed		Up to 3m/s
System Channel Bandwidth		10 MHz
Sampling Frequency (F_p)		11.2 MHz
FFT Size (NFFT)		1024
Sub-Carrier Frequency Spacing (f)		10.9375 kHz
Useful Symbol Time ($T_b = 1/f$)		91.4 μs
Guard Time ($T_g = T_b/8$)		11.4 μs
OFDMA Symbol Duration ($T_b + T_g$)		102.9 μs
Frame duration		5ms
Total Number of Data Symbols		47 (DL : UL = 31 : 16)
Power boosting of Pilot in DL PUSC		2.5dB
DL PUSC	Null Sub-carriers	184
	Pilot Sub-carriers	120 (40 per segment)
	Data Sub-carriers	720 (240 per segment)
	Sub-channels	30 (10 per segment)

2.2 Cell Layout

Figure 1 shows the N x N cell layout of the femtocell WiMAX systems in regular grids. Here N = 5 but it can be any positive integer. Each cell with generic square grid has an fBS in its center with a shift of (0.1m, 0.1m). Each fBS can be assigned one of three frequency segments. In Figure 1 all fBSs are assigned the same segment; such a system is called the single-segment system.

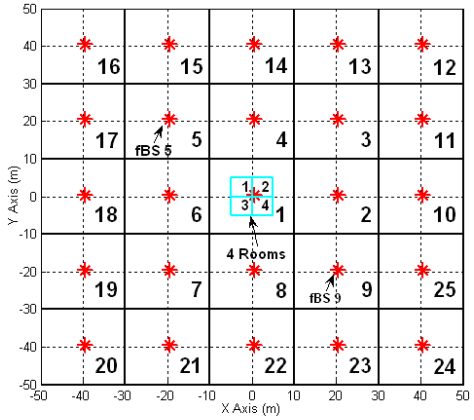

Figure 1. Femtocell WiMAX system in regular grids.

In center cell (Cell 1), four 5m-by-5m rooms are located around the center and fBS_1 is in the Room 2. So the house size is always 10m by 10m. We focus on the indoor MSs uniformly distributed in these rooms. By varying the cell radius R, we can have the houses with different distances when R > 5m (e.g., R = 10m as shown in Figure 1); and when R = 5m these "houses" are next to each other and hence correspond to "apartments".

Digital Object Identifier: 10.4108/ICST.WICON2008.4915
http://dx.doi.org/10.4108/ICST.WICON2008.4915

2.3 Channel Models

2.3.1 Path-Loss Model

The path loss types, usage models and detailed path-loss models are specified in [14, 15]. The different break-point distance (d_{BP}) is chosen in the following path loss model:

$$L(d) = \begin{cases} L_{FS}(d) = 20\log_{10}(4\pi d/\lambda), & d \le d_{BP} \\ L_{FS}(d_{BP}) + 35\log_{10}(d/d_{BP}), & d > d_{BP} \end{cases} \quad (1)$$

where d is the transmit-receive separation distance in meter and λ is the wavelength in meter. $L_{FS}(d)$ is the free space path loss with the distance of d. It is worth noting that with the introduction of d_{BP}, the minimum mean squared error (MMSE) estimator of the power law exponent n is 3.47, based on the measurement results in [3, 4].

The penetration attenuation is set as 5dB per wall between two rooms (5.4dB in [3]) for indoor links, while 10dB per wall for outdoor-to-indoor links.

2.3.2 Shadow Fading

According to [5], it is 5dB for indoor links and 10dB for outdoor links; and spatial correlation distance for indoor users is 5m.

2.3.3 Multi-path Fading

SISO multi-path channel models (A ~ F) are used for fBS–MS links according to the models specified in IEEE 802.11n [15], which are also listed in details in [16].

Two different models (B, F) are chosen for the indoor and outdoor links: Model B (2 clusters) is for a typical residential environment with 15ns root-mean-square (RMS) delay spread and further classified into B-LOS and B-NLOS. For B-LOS, the Ricean K-factor at the first delay is 10dB. Model F (6 clusters) is for a large open indoor/outdoor NLOS space with 150ns RMS delay spread.

Table 2 lists used propagation, multi-path fading and Log-normal fading models in the following simulation results.

Table 2. Femtocell channel models

Parameters		Type	Value
Propagation Model [14, 15]	Indoor links	B	d_{BP} = 5m
	Outdoor-to-indoor	F	d_{BP} = 30m
Penetration Path-Loss	Indoor links	B	5dB / wall
	Outdoor-to-indoor	B	10dB / wall
Multi-Path Fading [15, 16]	Intra-room links	B-LOS	0 ~ 80ns; K_0 =10dB (LOS)
	Room-to-room	B-NLOS	
	Outdoor-to-indoor	F	0 ~ 1050ns
Lognormal Fading [5]	Indoor links	B	5dB
	Outdoor-to-indoor	F	10dB

2.4 DL Partial Usage of SubChannels (PUSC)

While the 802.16 OFDMA PUSC permutation scheme is quite complex, it resembles random subcarrier permutation very well. Hence we approximate PUSC by using the approach specified in [1,17], which performs closely to standard PUSC.

2.5 DL CINR Calculation

Without loss of generality, we assume fBS_1 is assigned the 1st frequency segment (Segment 1). For a specific MS in center cell, its signal comes from fBS_1 and interferences come from the other fBSs with Segment 1. The CINR of the m-th subcarrier (γ_m) is:

$$\gamma_m = P_i \cdot |H_{i,m}|^2 \Big/ \left(\sum_{k=1,\, k\neq i}^{K} P_k \cdot |H_{k,m}|^2 + N_0 \right) \quad (2)$$

$$P_i = P_T G_i \cdot 10^{X_i/10} / L(d_i)$$

- P_i = received power at MS from fBS_i
- K = the number of cells (fBSs) with Segment 1
- N_0 = noise power
- P_T = TX power at each fBS
- G_i = antenna gain between the MS RX and fBS_i TX
- $H_{k,m}$ = the channel on the subcarrier m from fBS_k
- X_i = lognormal shadowing between the MS and fBS_i
- $L(d_i)$ = path loss at the MS from fBS i at distance d_i

The EESM method is used to convert the CINRs of individual subcarriers to the effective CINR of DL [18], defined as:

$$\gamma_{eff} = CINR_{eff} = -\beta \cdot \ln\left(\frac{1}{N} \sum_{m=1}^{N} \exp[-\gamma_m/\beta] \right) \quad (3)$$

- N is the number of subcarriers
- β, $\beta \ge 0$, is an EESM parameter

β is determined by the system configuration and modulation coding scheme (MCS), and can be obtained from the extensive link level simulations. Some important properties of EESM function can be found in [19]. Table 3 lists the MCS, their required Signal to Noise Ratio (SNR) and β values for DL. The β values of ITU PB model with speed of 3km/h in [20] are used.

Table 3. Modulation and coding scheme (MCS) in the DL

MCS (Repetition: default = 1)		Spectrum Efficiency	Receiver SNR (dB)	EESM β (dB)
QPSK	1/2 (4)	0.25	–2.50	2.18
	1/2 (2)	0.5	0.50	2.28
	1/2	1	3.50	2.46
	3/4	1.5	6.50	2.56
16QAM	1/2	2	9.00	7.45
	3/4	3	12.50	8.93
64QAM	1/2	3	14.50	11.31
	2/3	4	16.50	13.80
	3/4	4.5	18.50	14.71

3. SINGLE-SEGMENT SYSTEM

Two indices of system performance, system coverage and system capacity, are considered in this study. System coverage is defined as the probability that an MS randomly placed in the house has strong enough CINR to decode the DL preamble and MAP (transmitted with QPSK-1/2 with the repetition of 4). System capacity is defined as the total data rate per cell with the user (MS) resource fairness constraint.

Digital Object Identifier: 10.4108/ICST.WICON2008.4915
http://dx.doi.org/10.4108/ICST.WICON2008.4915

In this section we focus on the single-segment systems where all fBSs are assigned the same frequency segment. The MSs are uniformly distributed within the house. The effect of TX power at fBS, loading factor and cell radius are studied respectively.

3.1 Interference from an Individual fBS

Figure 2 shows the relative received interference power at the center fBS (fBS_1) from an individual interference fBS, as a function of their distance normalized by the cell size D, $D = 2 * R$. This individual interference power from fBS_i is calculated using the equation for P_i in (2), where $i \neq 1$ and fBS_i is in the same segment as fBS_1. The total interference power, which will be used later in Section 4, is simply the sum of all the individual interference power. Here the relative interference power is normalized by the interference power at the minimum distance D.

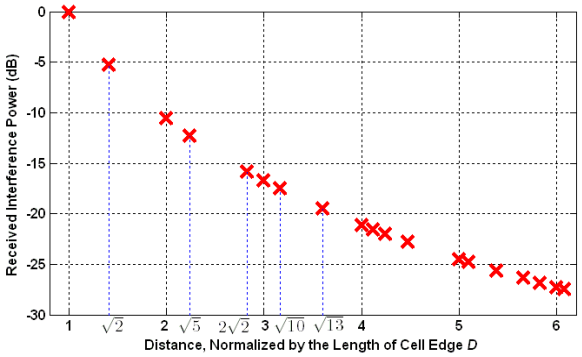

Figure 2. Received interference power from an individual fBS (relative to the maximum value) at different distances.

In Figure 2, the received interference power decreases rapidly. For example, from D to $3D$ of the distance, this reduction is 16.7dB. Since the dominance of the interference fBS at the short distance can be clearly observed, to simplify the system performance simulation, a 5x5 cell layout is considered in the system-level performance analysis. That is, for the target fBSs (fBS_1 in Figure 1), only the interference sources from the neighboring 1st and 2nd tiers of fBSs (fBS_1 ~ fBS_{25} in Figure 1) are considered. This 5x5 cell layout can provide an approximation of the larger layouts with acceptable errors.

3.2 Effect of TX Power at fBS

Consider all fBSs with the same TX power (P_T). The case where fBSs have heterogeneous TX powers is beyond the scope of this paper. Figure 3 shows the DL system performance, in terms of system coverage and capacity, versus fBS TX power (14, 17, 23dBm) under different setups of the cell radius (5, 10, 20m) and loading factor (20%, 60%, 100%).

As shown in Figure 3, in terms of system coverage and capacity the single-segment system always has almost the same performance, regardless of the fBS TX power. In other words, the fBS TX power does not play a significant role at all. This is because the system interference caused by receiver noise is overwhelmed by the interference from adjacent fBSs. The effect of increased signal power and interference power simply cancel each other. Since the considered system performances are independent of the fBS TX power, we fix the fBS TX power as 17dBm for the rest of this paper.

It is worth noting that TX power still plays an important role for the noise limited isolated single-cell case. It affects the link budget and coverage range.

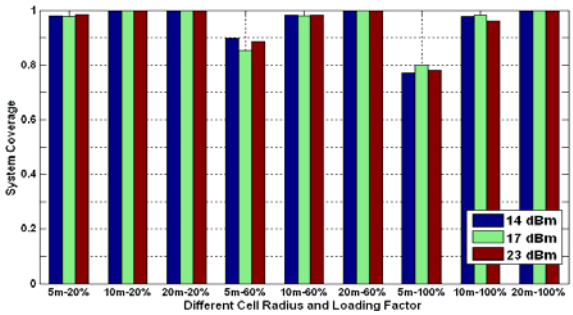

(a) DL System Coverage

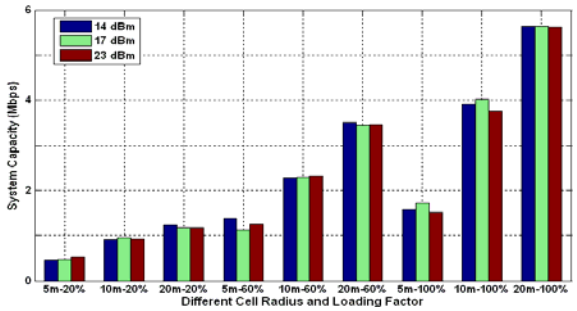

(b) DL System Capacity per Cell (Mbps)

Figure 3. Effect of fBS TX power in single-segment systems with 2:1 DL:UL partitioning.

3.3 Effect of Cell Radius and Loading Factor

Figure 4 shows the DL system coverage and capacity under different setups of the cell radius (5, 10, 20m) and loading factor (20%, 40%, 60%, 80%, 100%) with a fixed P_T of 17dBm. The case of single cell is equivalent to the cell radius of ∞ with no interference from adjacent cells.

As shown in Figure 4, with the increase of the cell size, the fBSs move away from each other and hence generate less interference to each other, which leads to a higher system performance.

Unlike the cell radius, the loading factor has a more complicated effect on the system performance. In Figure 4(a), increased loading factor reduces the system coverage because higher system load represents statistically more overlapping of subcarriers in different cells and stronger interference between the neighboring femtocells assigned to the same frequency segment. On the other hand, system capacity is an increasing function of loading factor in Figure 4(b). This is because the system utilizes more subcarriers but only suffers a slight decrease of network coverage, which in combination leads to increased capacity.

Figure 5 shows an instance of the indoor coverage area (10m by 10m) in a single simulated frame under different cell radius and loading factor. The color in each small rectangular represents the highest supportable MCS for the MSs within the area. Yellow areas are not covered by any MCS. Red areas are covered only by QPSK ½ with repetition 4. Blue areas are covered by 64QAM ¾. The areas of various combined intensities of red and blue are covered by MCS levels in between.

Digital Object Identifier: 10.4108/ICST.WICON2008.4915
http://dx.doi.org/10.4108/ICST.WICON2008.4915

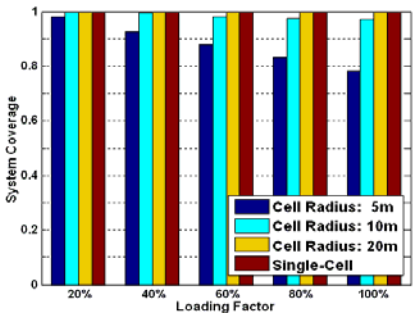

(a) DL System Coverage

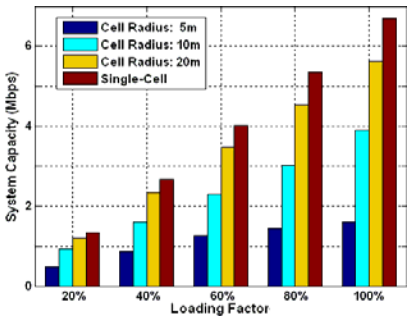

(b) DL System Capacity per Cell (Mbps)

Figure 4. Effect of the cell radius and loading factor in single-segment systems with 2:1 DL:UL partitioning.

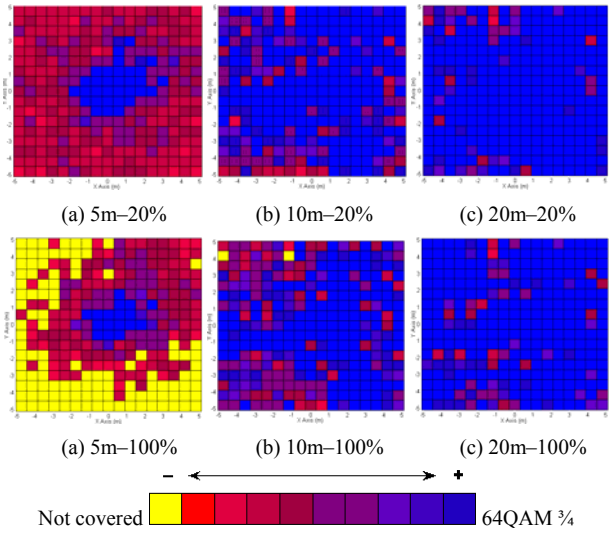

Figure 5. Network coverage for indoor MSs in a single simulated frame. Different colors represnet the highest MCS supported for the MSs in the area.

Assume the minimum performance requirement is to provide 95% DL coverage and 1Mbps DL capacity,[1] respectively. From Figure 3 ~ 5, the single-segment system cannot meet both of these performance requirements for some cases when the cell radius is 5m and/or the loading factor is 20%. So we need to study the performance of practical systems with frequency segment assignment schemes.

4. FREQUENCY ASSIGNMENT SCHEMES AND NETWORK SELF ORGANIZATION

The scenario studied in the last section where all fBSs transmit the same frequency segment represents the worst-case scenario. To further the study of practical systems, we consider the frequency assignment schemes, which can improve the system performance by reducing the inter-cell interference to acceptable levels.

We focus on the frequency assignment schemes in the self-organizing of femtocell network context. The simplest frequency assignment scheme is Random Scheme, in which each fBS randomly selects one out of three segments without any measurements or communication with the network controller. It is used here as a baseline for comparison with other algorithms. Several heuristic greedy-based schemes are proposed and compared with Random Scheme in this section.

4.1 Optimum Pattern (OPTM)

Optimum Pattern (*OPTM*) avoids assigning the same frequency segment to two immediate adjacent fBSs. Each marker (color) represents a different frequency segment. For the regular square topology we study here, Figure 6 shows the optimal frequency assignment in a 20 x 20 cell layout.

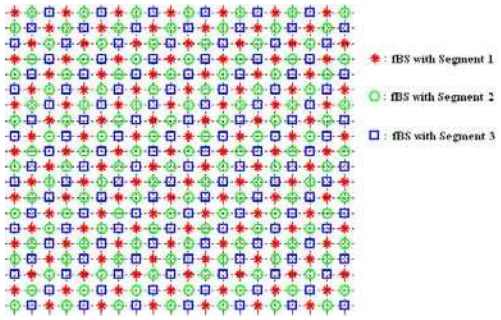

Figure 6. Optimum pattern (circular shift pattern).

In Figure 6, from the bottom to the top, the formed pattern in each row is exactly a circular shift of its previous row with one shift to the right. The similar facts are observed for columns. So Optimum Pattern is also called Circular Shift Pattern. Define the inner fBS as the one that is not at or close to the edges of the layout. In Figure 6, without consideration of the edge effect, the system topology with frequency assignment patterns is identical from the viewpoint of arbitrary inner fBS.

In Optimum Pattern, the segment assignment of any fBS is pre-determined by the network controller based on the geographic topology of the whole network even before the turn-on of this fBS. However, Optimum Pattern cannot be implemented when the geographic topology is unknown; instead, alternative schemes need to be considered: each fBS is assigned the segment by the network controller according to the measurements of itself and its neighboring cells.

[1] This 1Mbps (DL) system can support up to four 12.2kbps voice users, four 64kbps data users, two 144kbps data users and one 384kbps data user simultaneously.

Digital Object Identifier: 10.4108/ICST.WICON2008.4915
http://dx.doi.org/10.4108/ICST.WICON2008.4915

4.2 General Algorithm and Heuristic Schemes

Figure 7 depicts the general algorithm for arbitrary frequency assignment scheme, including Random Scheme and any heuristic scheme. In our simulations, M is set as 105 and M^2 is the total cell numbers in the system. For the same turn-on order of fBSs, different schemes only have different decision rules at Step 2.1.

1. Input: the turn-on order of all fBSs in M x M cells.
2. Each time an fBS is turned on,
   - 2.1. It is assigned one of the 3 frequency segments based on the specified frequency assignment scheme; and if necessary the following tiebreak rules are used:
   - 2.2. Pick the one with the least number of fBSs among the tied segments; and if a tie still exists,
   - 2.3. Randomly pick one of the tied segments.

Figure 7. General algorithm of frequency assignment schemes.

Performance of each frequency assignment algorithm is evaluated using some randomly picked 5x5 cells layout. Edges of the network are avoided to reduce the edge effect. To describe the heuristic schemes, we have the following denotations: Denote Ξ as the complete set of all the existing turned on fBSs. j, $k \in \Xi$, meaning that fBS_j and fBS_k have been turned on. Let fBS_m be the newly turned on fBS, hence $m \notin \Xi$. i, i = 1, 2, 3, is the index of an available frequency segment. $S(j) = i$ means that Segment i is assigned to fBS_j. N_i is the number of fBSs that have been assigned to Segment i. P_{jk} is the received power at fBS_j from fBS_k, regardless of whether fBS_j and fBS_k are in the same segment or not. For convenience, we set $P_{jj} = 0$. δ_{jk} is an indicator parameter: $\delta_{jk} = 1$ if fBS_j and fBS_k are in the same segment; 0 otherwise. $S(m)$, P_{jm} and δ_{jm} have the similar meanings as $S(j)$, P_{jk} and δ_{jk}, respectively, except that the newly turned on fBS_m is involved.

4.2.1 Min-Max Individual Interference Power (Min-Max) Scheme

For Min-Max Individual Interference Power (*Min-Max*) scheme, at Step 2.1 in Figure 7, the newly turned on fBS_m is assigned the segment $S^*(m)$ that minimizes the maximum interference generated between any pair of two fBSs assigned to this segment. It can be written as:

$$S^*(m) = \arg\min_{S(m)=1,2,3} \left[\max_{j,k \in \Xi} \left(P_{jk}\delta_{jk}\delta_{jm},\ P_{jm}\delta_{jm} \right) \right]. \quad (4)$$

In practice, the received interference power between any two fBSs in the same segment can be measured at their RX, and reported to the network controller for decisions based on *Min-Max* scheme.

4.2.2 Min Average Total Interference Power (MATIP) Scheme

For Min Average Total Interference Power (*MATIP*) scheme, at Step 2.1 in Figure 7, the newly turned on fBS_m is assigned the segment $S^*(m)$ that minimizes the average total interference power received at the individual fBS over all fBSs assigned to this segment. It can be written as:

$$S^*(m) = \arg\min_{S(m)=1,2,3} \frac{\sum_{j,k \in \Xi} \left(P_{jk}\delta_{jk}\delta_{jm} \right) + 2 \cdot \sum_{j \in \Xi} \left(P_{jm}\delta_{jm} \right)}{N_{S(m)} + 1}. \quad (5)$$

In practice, the number of fBSs in each segment is known by the network controller; and the received total interference power at each fBS can be measured and reported to the controller for decisions based on *MATIP* scheme.

4.2.3 Least Interference Power (LIP) Scheme

For Least Interference Power (*LIP*) scheme, at Step 2.1 in Figure 7, the newly turned on fBS_m is assigned the segment $S^*(m)$ that minimizes the received total interference power (i.e., maximizes the received CINR) at RX of the new fBS. It can be written as:

$$S^*(m) = \arg\min_{S(m)=1,2,3} \left[\sum_{j \in \Xi} \left(P_{jm}\delta_{jm} \right) \right]. \quad (6)$$

In practice, *LIP* scheme only requires that each fBS reports its received CINR in each segment to the network controller. This information is completely local to this fBS and does not demand any computation at all.

4.3 Turn-on Orders of fBSs

The turn-on order of fBSs considered here is equivalent to the sequence of frequency assignment applied to these fBSs. From our previous discussion, *Min-Max*, *MATIP* and *LIP* schemes are greedy schemes and their performance would depend on the turn-on order of the fBSs. The turn-on orders can be classified into two types: the fixed ones and the randomized ones.

4.3.1 Fixed Turn-on Orders of all fBSs

The fixed turn-on order adopted here is as follows: the fBSs are turned on row by row in one direction (assumed from the bottom to the top); within each row, all fBSs are turned on in the same direction (assumed from the leftmost to the rightmost).With this fixed turn-on order, each newly turned on fBS has the chance to choose a segment different from its immediate neighbors that are only located in its bottom and/or left.

Note that the Random Scheme and the Optimum Pattern are independent of the turn-on orders. To evaluate the performance of its frequency assignments, each heuristic scheme has been simulated for 1000 runs with the above fixed turn-on order in the 105x105 cell layout according to the general algorithm described in Figure 7.

After each simulation run of the frequency assignments with any specific scheme, 10 clusters (each cluster consists of 5x5 inner cells) are randomly picked to compute the received interference power at the typical fBS. The average total interference power, associated with the specific heuristic scheme, is used as a performance metric to compare the different heuristic schemes with the fixed turn-on order, as shown in Figure 8.

Random Scheme is also shown in Figure 8 as a comparison basis. The average interference power of any other scheme is normalized over that of Random Scheme, which is set as 0dB. It is demonstrated that with the fixed turn-on order, *MATIP* and *LIP* schemes are all exactly Optimum Pattern, which has around 3.6dB improvement of CINR compared with Random Scheme.

Digital Object Identifier: 10.4108/ICST.WICON2008.4915
http://dx.doi.org/10.4108/ICST.WICON2008.4915

Even *Min-Max* scheme provides a 2.4dB improvement of CINR over Random Scheme.

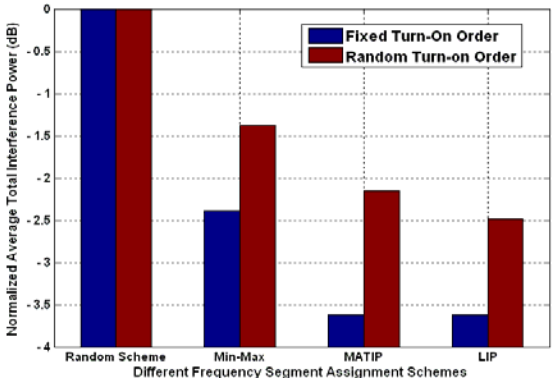

Figure 8. Comparison of frequency assignment schemes: average received total interference power.

4.3.2 Randomized Turn-on Orders of all fBSs

While the fixed turn-on order can be considered as applying frequency assignments to all of fBSs with known geographic topology at once, randomized turn-on order is considered as applying frequency assignments to fBSs sequentially in the same order of the time when they are powered on. The randomized turn-on order represents a more realistic situation in which femtocells are added to the network in a random order.

Similarly to Section 4.3.1, the average received total interference power at the center fBS, obtained based on randomly picked 5x5 cells clusters in the network, is associated with the specific heuristic scheme. Figure 8 compares different heuristic schemes in term of the above performance metric.

In Figure 8, Random Scheme is independent of the turn-on orders. With the random turn-on orders, *MATIP* and *LIP* schemes have a performance degradation of 1.5dB and 1.1dB from the Optimum Pattern, respectively. However, they still have around 2.1dB and 2.5dB improvement, respectively, compared with Random Scheme.

The resulted frequency assignments in each of 10,000 5x5 cells, with either fixed or randomized turn-on orders of all fBSs, are also recorded for the system-level simulations in Section 4.4. It is worth noting that with only a subset of all fBSs being turned on, any irregular cell layout can be approximated and simulated using our cell layout in regular grids.

4.4 SYSTEM-LEVEL PERFORMANCE COMPARISON

In this section, the system-level simulation approach described in Section 3 is conducted to compare different frequency assignment schemes in terms of system coverage and capacity.

4.4.1 Simulation Setups

The 5x5 cell layout is used. All 25 fBSs have the same TX power P_T = 17dBm and the system is always fully loaded (i.e., the loading factor is 100%). The considered cell radii are 5, 10 and 20m in general, but for the single-segment system the cell radii of $5\sqrt{2}$, $10\sqrt{2}$, $20\sqrt{2}$ and 40m are simulated as well.

The MSs are uniformly distributed with 0.5m spacing in the center cell. The frequency assignments of all 25 fBSs are determined based on the recorded results of Section 4.3. For these greedy schemes: *Min-Max*, *MATIP* and *LIP* scheme, only the randomized turn-on orders are considered.

The other system parameters and models are given in Section 2. For each scheme, a number of different frequency assignments are simulated and the system-level performance metrics are obtained by averaging over these different instances.

4.4.2 System Coverage and Capacity

Figure 9 compares the system coverage and capacity of different heuristic frequency assignment schemes with the randomized turn-on order, as well as Random Scheme and Optimum Pattern.

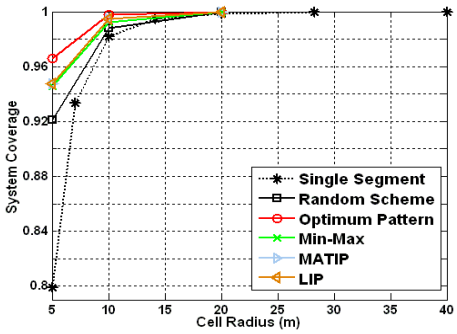

(a) DL System Coverage

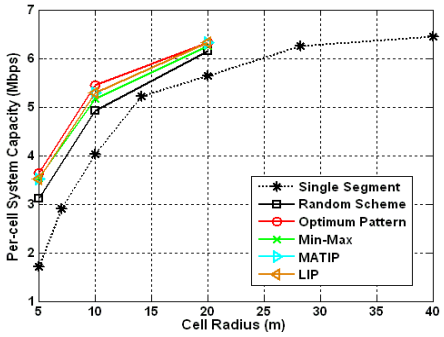

(b) DL System Capacity (per-cell)

Figure 9. Comparison of frequency assignment schemes: DL system coverage and capacity with 2:1 DL:UL partitioning.

In Figure 9, the single-segment system is the worst scenario. And the Random Scheme provides the lower bound for realistic frequency assignment schemes. The system coverage is not an issue because it is at least 92% even for the fully loaded system with the 5m cell radius. On the other hand, Optimum Pattern, plotted as the lines with circular markers, always has the best performance in Figure 9. The three greedy schemes lie between Random Scheme and Optimum Pattern. Among them, *MATIP* and *LIP* schemes are very close to each other and perform better than *Min-Max* scheme.

With a 20m cell radius, i.e., a relative large distance between the neighboring fBSs, Random Scheme and Optimum Pattern (and all other heuristic schemes in the between) have 100% system coverage and almost the same capacity with only a 0.3Mbps difference. However, with a 5m or 10m cell radius, the fBSs are crowded; Optimum Pattern has a 0.6Mbps capacity improvement

Digital Object Identifier: 10.4108/ICST.WICON2008.4915
http://dx.doi.org/10.4108/ICST.WICON2008.4915

(16% or 11% increase at 5m or 10m cell radius, respectively) compared with Random Scheme. In these cases, *MATIP* and *LIP* schemes have the capacity of around 0.45Mbps higher than that of Random Scheme.

The system-level performance comparison of different frequency assignment schemes here is consistent with the results we have in Section 4.2 where the considered metric is the received total interference power. Hence, the final conclusions can be drawn as follows: the proposed heuristic schemes can improve the system performance, especially *MATIP* and *LIP* schemes, which perform closely to Optimum Pattern in terms of system coverage and capacity; and among all schemes, *LIP* scheme is the best one because it utilizes only the local information (the received CINR at the fBS itself) that is always available, and demands no computation (comparisons only).

4.5 Frequency Segment Assignment Schemes with the Reassignment Algorithm (RA)

In Figure 8, compared with the Optimum Pattern, the *LIP* scheme with random turn-on orders has 1.1dB performance degradation in term of the average received total interference power. This 1.1dB gap also leads to a 0.1 ~ 0.2dB difference in their DL system capacity, as shown in Figure 9. To reduce this gap, we propose an event-driven reassignment algorithm as shown in Figure 10. This reassignment algorithm can work with an arbitrary frequency assignment scheme. In this paper we evaluate the event-driven reassignment algorithm on top of three heuristic schemes introduced in Section 4.2, i.e. *Min-Max*, *MATIP* and *LIP* scheme. The resulted schemes with reassignments are called *Min-Max-RA*, *MATIP-RA* and *LIP-RA* scheme, respectively.

1 Input: the turn-on order of all fBSs in M x M cells and two given interference power thresholds, P_0 and P_1.

2 When fBS_m is turned on, it is assigned segment $S^*(m)$ based on the specified frequency assignment scheme in Section 4.2.

3 The reassignment algorithm is triggered if and only if the received interference power at fBS_m from any individual fBS_j in the segment $S^*(m)$ is beyond the threshold P_0, i.e.,

$$\exists\, j \in \mathbf{\Xi},\ P_{jm}\delta_{jm} \geq P_0 .\ .$$

3.1 The set of to-be-reassigned fBSs, $\mathbf{\Theta}$, includes fBS_m and its closest neighbors, regardless of whether they are in the same segment as fBS_m or not, i.e.,

$$\mathbf{\Theta} = \{m\} \cup \{j \in \mathbf{\Xi} : P_{jm} \geq P_1\} .$$

Note the information of P_{jm} may be obtained during the initial assignment process of fBS_m.

3.2 Denote $\mathbf{\Omega}$, $\mathbf{\Omega} = \{\omega\}$, as the complete set of all feasible reassignments for all fBSs in $\mathbf{\Theta}$. Pick the reassignment ω^* for $\mathbf{\Theta}$ that minimizes the sum of total interference power received at all fBSs in $\mathbf{\Theta}$, as

$$w^* = \arg\min_{\omega \in \mathbf{\Omega}} \left[\sum_{j \in \mathbf{\Theta}} \sum_{k \in \mathbf{\Xi}} \left(P_{jk}\delta_{jk}^{\omega} + P_{jm}\delta_{jm}^{\omega} \right) \right],$$

where δ_{jk}^{ω} is the indicator parameter based on the reassignment ω.

Figure 10. Arbitrary frequency assignment scheme with the event-driven reassignment algorithm.

In Figure 10, P_0 represents the interference power threshold which triggers the reassignments, while P_1 is the received power threshold utilized to select the fBSs for reassignments. These two parameters are tunable and universal to all fBSs. In this paper, $P_0 = P_1$ and are set as the corresponding individual interference power between two immediate neighbors in the same segment at the distance D.

In the step 3 of Figure 10, the reassignment algorithm is triggered when the newly turned on fBS (fBS_m) falls into a "crowded" zone with a number of existing turned on fBSs in all three segments. This situation occurs due to the randomness of turn-on order. In the step 3.1, a small group of fBSs, consisting of fBS_m and its turned on immediate neighbors, are selected for reassignments. The exhaustive search of final reassignments in the step 3.2 considers all the feasible assignments to the selected small group of fBSs in step 3.1, and selects the assignment ω^* which minimizes the total interference experienced by all fBSs in the set $\mathbf{\Theta}$. The search over all possible frequency assignments in the set $\mathbf{\Omega}$ is possible because of the relative small size of $\mathbf{\Theta}$ (typically no more than 5 in our simulations).

It is worth noting that unlike *LIP* scheme, *LIP-RA* scheme uses not only the received CINR at fBS_m, but also the received power at fBS_m from each of its closest neighboring fBSs. This increases the required information exchange between fBS_m and the network controller; however, this additional information exchange is limited due to that only a small group of fBSs surrounding fBS_m (inclusively) are involved in the reassignments. Also, the required information is available at fBS_m itself. Therefore, *LIP-RA* scheme in some sense is still based on limited local information and demands not much computation.

Figure 11 shows the performance study of the *Min-Max-RA*, *MATIP-RA*, and *LIP-RA* schemes, in term of the previous metrics adopted in Figure 8 and Figure 9. As shown in Figure 11(a), compared with its original scheme without reassignments in term of the average received total interference power, *Min-Max-RA* has a 1.1dB improvement, the most among three heuristic schemes; and *LIP-RA* scheme provides a 0.3dB improvement, which leaves a 0.8dB gap to the Optimum Pattern but still better than any other scheme. In addition, as shown in Figure 11(b) and (c), *LIP-RA* scheme outperforms *LIP*, *Min-Max-RA* and *MATIP-RA* scheme in term of DL system coverage and capacity, although for some cases their difference is not significant.

5. CONCLUSIONS

In this paper, the DL performance of the WiMAX (802.16e) femtocell systems in regular grids is evaluated in terms of the network coverage and the system capacity for the indoor MSs. The single-segment systems without any frequency assignment scheme are considered at first. It has been demonstrated through extensive simulation that the system coverage and capacity are independent of the TX power at fBSs. The effect of the cell radius and loading factor is also investigated respectively. Furthermore, several heuristic frequency assignment schemes are proposed as network self-optimization schemes and compared along with the random assignment scheme that randomly assigns one of three segments for each fBS. Finally we draw our conclusion that Least Interference Power (*LIP*) scheme is the best practical scheme

Digital Object Identifier: 10.4108/ICST.WICON2008.4915
http://dx.doi.org/10.4108/ICST.WICON2008.4915

among them due to its complete locality, practical metric (the received CINR), no computation needed and its close-to-optimum system performance. An event-driven Reassignment Algorithm (*RA*) is proposed as an addition to arbitrary frequency assignment scheme to further improve the system performance.

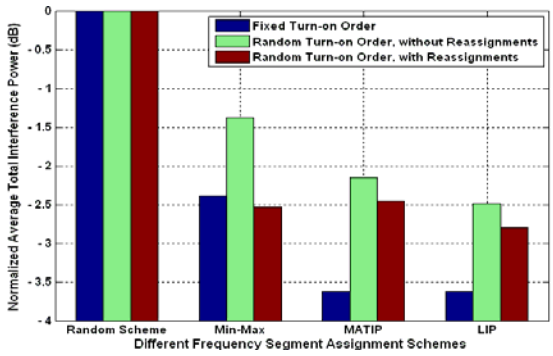

(a) Average Received Total Interference Power

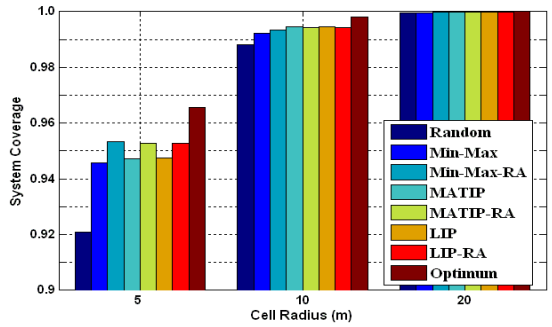

(b) DL System Coverage

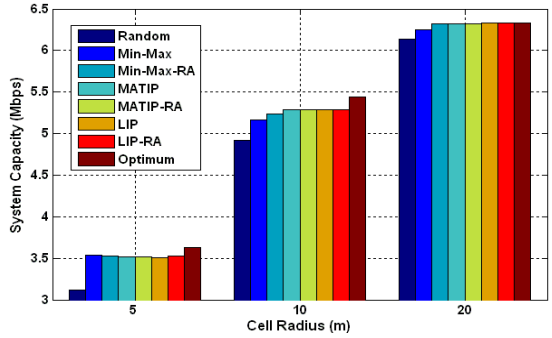

(c) DL System Capacity (per-cell)

Figure 11. Performance study of the reassignment algorithm: average received total interference power, DL system coverage and capacity with 2:1 DL:UL partitioning

6. REFERENCES

[1] "WiMAX System Evaluation Methodology", Version 2.0.1, WiMAX Forum, December 15, 2007.

[2] M. Feuerstein, K. Blackard, T. Rappaport, et al., "Path loss, delay spread, and outage models as functions of antenna height for microcellular system design", IEEE Trans. on Vehicular Technology, Vol. 43, No. 3, August 1994.

[3] C. Anderson and T. Rappaport, "In-building wideband partition loss measurements at 2.5 and 60 GHz", IEEE Trans. on Wireless Communications, Vol. 3, No. 3, May 2004.

[4] C. Anderson, T. Rappaport, K. Bae, et al., "In-building wideband multipath characteristics at 2.5 & 60 GHz", 56th IEEE Vehicular Technology Conference, Vol. 1, pp. 97–101, Vancouver, Canada, 2002.

[5] A. Pace and L. Valentini, "System level performance evaluation of UTRA-FDD (UMTS Terrestrial Radio Access – Frequency Division Duplex) ", PIMRC 2000, Vol. 1, pp. 343–347, 2000.

[6] P. Nobles and F. Halsall, "Indoor propagation at 17GHz and 60GHz – measurements and modeling", IEE National Conference on Antennas and Propagation, York, UK, 1999.

[7] D. Cox and D. Reudnik, "A Comparison of Some Channel Assignment Strategies in Large-Scale Mobile Communications Systems", IEEE Trans. on Comm., Vol. COM-20, No. 2, pp. 190-195, Apr. 1972.

[8] T. Takenata, T. Nakamura and Y. Tajima, "All Channel Concentric Allocation in Cellular Systems", Proc. IEEE ICC, pp. 920-924, Geneva, May 1993.

[9] H. Salgado, M. Sirbu and J. Peha, "Spectrum Sharing Through Dynamic Channel Assignment for Open Access to Personal Communications Services", Proc. IEEE ICC, pp. 417-422, June 1995.

[10] X. Fu, Y. Pan, A. G. Bourgeois and P. Fan, "A Three-Stage Heuristic Combined Genetic Algorithm Strategy to the Channel-Assignment Problem", Proc. IEEE IPDPS'03, pp. 145-152, 2003.

[11] K. N. Sivarajan, R. J. McEliece and J. W. Ketchun, "Channel Assignment in Cellular Radio", Proc. 39th IEEE Vehicular Technology Conference, pp. 846-850, May 1989.

[12] C. Prehofer and C. Bettstetter, "Self-Organization in Communication Networks: Principle and Design Paradigms", IEEE Comm. Magazine, Vol. 43-7, pp. 78-85, July 2005.

[13] IEEE Standard 802.16e: "Air Interface for Fixed and Mobile Broadband Wireless Access Systems" with Amendment 2: "Physical and Medium Access Control Layers for Combined Fixed and Mobile Operation in Licensed Bands" and Corrigendum 1.

[14] "Usage Models", IEEE 802.11n Working Group, IEEE 802.11-03/802r14, 03/16/2004.

[15] "Indoor MIMO WLAN Channel Models", IEEE 802.11n Working Group, IEEE 802.11-03/162r2, 07/11/2003.

[16] A. Botonjic, "MIMO Channel Models", Master thesis, University of Linköping, Sweden, January 30, 2004.

[17] A. Maltserv, et al. "PUSC Permutation Analysis in Interference Environment", Rev 0.4, April 2005.

[18] "CINR measurement using EESM method", IEEE 802.16 Working Group, IEEE 80216e-05/141r3, 04/29/2005.

[19] H. Zeng and C. Zhu, "System-Level Modeling and Performance Evaluation of Multi-hop 802.16j Systems", IWCMC 2008, Crete Island, Greece, August 2008.

Digital Object Identifier: 10.4108/ICST.WICON2008.4915
http://dx.doi.org/10.4108/ICST.WICON2008.4915

[20] Beijing University of Post and Telecommunication, "EESM Beta Training in 802.16e System", WiMAX Forum AATG, August 17, 2007.

Digital Object Identifier: 10.4108/ICST.WICON2008.4915
http://dx.doi.org/10.4108/ICST.WICON2008.4915